The Cryosphere
Discussions

Open Access

EGU

1 **Spatial and temporal variability of sea-salts in ice cores**

2 **and snow pits from Fimbul Ice Shelf, Antarctica**

3 Carmen Paulina Vega,[1,2,¶,§] Elisabeth Isaksson,[1] Elisabeth Schlosser,[3,4] Dmitry

4 Divine,[1] Tõnu Martma,[5] Robert Mulvaney,[6] Anja Eichler,[7] and Margit Schwikowski.[7]

5 [1]{Norwegian Polar Institute, N-9296 Tromsø, Norway}

6 [2]{Department of Earth Sciences, Uppsala University, Villavägen 16, SE-752 36,

7 Uppsala, Sweden}

8 [3]{Institute of Atmospheric and Cryospheric Sciences, University of Innsbruck,

9 Innsbruck, Austria}

10 [4]{Austrian Polar Research Institute, Vienna, Austria}

11 [5]{Department of Geology, Tallinn University of Technology, Tallinn, Estonia}

12 [6]{British Antarctic Survey, Madingley Road, High Cross, Cambridge,

13 CambridgeshireCB3 0ET, United Kingdom}

14 [7]{Paul Scherrer Institute, 5232 Villigen PSI, Switzerland}

15 Now at:

16 [¶] {School of Physics, University of Costa Rica, San Pedro de Montes de Oca,

17 11501-2060 San Jose, Costa Rica}

18 [§] {Centre for Geophysical Research, University of Costa Rica, San Pedro de

19 Montes de Oca, 11501-2060 San Jose, Costa Rica}

20 Correspondence to: C. P. Vega (carmen.vegariquelme@ucr.ac.cr)

21 **Abstract**

22 Major ions were analysed in three firn cores from different ice rises located at Fimbul

23 Ice Shelf (FIS): Kupol Ciolkovskogo (KC), Kupol Moskovskij (KM), and Blåskimen

24 Island (BI), a 100 m long core drilled near the FIS edge (S100), and five snow pits

25 (M1, M2, G3, G4, and G5) sampled on the ice shelf. These sites are distributed over

26 the entire FIS area so that they provide a variety of elevation and distance to the

27 sea. Sea-salt species (mainly Na^+ and Cl^-) generally dominate the precipitation

28 chemistry in the study region. Concentrations of these ions were found to decrease

29 with latitude and distance from the sea. We associate a significant six-fold increase

1

1 in sea-salts observed in the S100 core after the 1950s with a change in deposition

2 regime. This increase in sea-salt concentrations is synchronous with a shift in non-

3 sea-salt sulfate ($nssSO_4^{2-}$) toward negative values, suggesting a possible

4 contribution of fractionated aerosol to the sea-salt load in the S100 core most likely

5 by dry deposition. In contrast, wet deposition of atmospheric sea-salts is dominant

6 in the three ice rises cores, and no evidence of a significant contribution of

7 fractionated sea-salt to these sites was found. In summary, these results suggest

8 that the S100 core contains a more local sea-salt signal, dominated by processes

9 during sea-ice formation in the neighbouring waters. In contrast, the ice rises cores

10 register the larger-scale signal of atmospheric flow conditions and transport of sea-

11 salt aerosols produced over open water rather than local changes in sea-ice, wind-

12 blown snow accumulated over sea-ice, and frost flower formation. These findings

13 are a contribution to the understanding of the mechanisms behind sea-salt aerosol

14 production, transport and deposition at coastal Antarctic sites, and for the

15 improvement of the current Antarctic sea-ice reconstructions based on sea-salt

16 chemical proxies obtained from ice cores.

17 **1 Introduction**

18 Antarctic ice and firn cores contain valuable information about the climate and

19 atmospheric chemical composition of the past and provide evidence for the

20 important role of Antarctica in the global climate system. Numerous ice and firn

21 cores have been drilled in Antarctica during the past decades (Stenni et al., 2017).

22 However, relatively few cores were drilled in coastal regions, which are more

23 sensitive to changes in climate than the dry and cold interior of Antarctica. In fact,

24 two recent review papers point out the lack of ice core data from low elevation

25 coastal areas when discussing Antarctic climate variability (Stenni et al., 2017;

26 Thomas et al., 2017). In an effort to understand the role of ice shelves in stabilizing

27 the Antarctic ice sheet, particular focus has been laid on the investigation of ice rises

28 and ice rumples as buttressing elements within the ice sheet - ice shelf complex

29 (Paterson, 1994; Matsuoka et al., 2015). Furthermore, due to their radial ice flow

30 regime, generally low ice velocities, and relatively high surface mass balance

31 (SMB), ice rises are potentially useful sites for ice core retrieval (Philippe et al., 2016;

The Cryosphere

Discussions

1   Vega et al., 2016). Firn and ice cores drilled at ice rises allow obtaining high-

2   resolution climate records to investigate subannual and long-term temporal changes

3   in the loads of different chemical compounds found in the snow, providing

4   information about their sources and transport, particularly of sea-salt ions, such as

5   sodium (Na^+) and chloride (Cl^-), which are strongly modulated by sea-ice extent and

6   meteorological conditions. Recent modelling efforts to study the use of sea-salts as

7   proxies for past sea-ice extent have shown that, under present climate conditions

8   and on interannual timescales, meteorological conditions rather than sea-ice extent

9   are the dominant factor modulating atmospheric sea-salt concentrations that are

10   deposited at the interior and coastal sites in Antarctica (Levine et al., 2014).

11   However, sea-salts have the potential as proxy for sea-ice extent at glacial-

12   interglacial scales when large changes in sea-ice extent took place (Levine et al.,

13   2014).

14   At most Antarctic sites, atmospheric sea-salt concentrations present maxima during

15   austral winter (Wagenbach et al., 1998; Weller and Wagenbach, 2007; Jourdain et

16   al., 2008; Udisti et al., 2012), with the exception of Dumont D'Urville where maxima

17   occur during summer (Wagenbach et al., 1998). Similarly, sea-salt fluxes obtained

18   from Antarctic ice cores also show winter maxima (Abram et al. 2013 and references

19   therein). However, in some recent core records from coastal sites no clear

20   seasonality is observed, e.g. at Mill Island during the period 1934–2000 (Inoue et

21   al., 2017). Abram et al. (2013) conclude that despite the seasonal signal registered

22   in different Antarctic ice cores, sea-salt fluxes do not show a consistent relationship

23   with sea-ice extent on interannual timescales, and on the contrary, are highly

24   dependent on atmospheric transport, and/or the presence of polynyas.

25   Hitherto, two main sources of increased winter sea-salt aerosols have been

26   proposed: (i) increased storminess leading to an enhancement of sea-salt aerosols

27   above the open ocean with possibly faster meridional transport (Petit et al., 1999;

28   Fischer et al. 2007), and (ii) a direct input of sea-salts associated to increases in

29   sea-ice, overcoming source (i), e.g. due to frost flowers (Rankin and Wolff, 2002,

30   2004; Roscoe et al., 2011), brine (Rankin et al., 2000), and the contribution of snow

31   transported over sea-ice by wind (Yang et al., 2008, 2010; Huang and Jaeglé, 2017).

1   In the review by Abram et al. (2013), the authors suggest that the brine-frost flower

2   system is a plausible source of sea-salt aerosols to coastal Antarctic sites. This

3   evidence consists of negative non sea-salt sulfate ($nssSO_4^{2-}$) values both in winter

4   aerosol and fresh snow sampled at coastal sites (Hall and Wolff, 1998; Wagenbach

5   et al., 1998; Curran et al., 1998; Rankin and Wolff, 2002; and Rankin and Wolff,

6   2003), and also in ice cores from both inland (Wagenbach et al., 1994, Kreutz et al.,

7   1998) and coastal sites (Inoue et al., 2017). These negative values suggest that the

8   sea-salt source was highly fractionated compared to seawater.

9   During the process of sea-ice formation, ions present in the water are not

10 incorporated in the ice crystal matrix, but remain as highly concentrated brine in

11 brine pockets or channels. The brine can be transported by capillary effects through

12 brine channels to the newly formed ice surface, resulting in a thin layer of highly

13 saline surface brine. This fractionated brine is unlikely to be a direct source of sea-

14 salts because it usually quickly gets covered by snow or frost flowers, and no clear

15 mechanism has been found to explain how this brine could become airborne (Abram

16 et al., 2013). With further cooling of the ice, the volume of brine decreases and

17 consequently, its salinity increases, leading to the precipitation of different saline

18 compounds. This depends on the temperature, e.g. sodium sulfate or mirabilite

19 ($Na_2SO_4 \cdot 10\,H_2O$) starts to precipitate at temperatures below -8 °C, and sodium

20 chloride (NaCl) at temperatures below -26 °C. Consequently, the remaining brine is

21 depleted in sodium and sulfate ions via precipitation of mirabilite at relatively mild

22 polar temperatures. Frost flowers can form from this brine when meteorological

23 conditions are adequate, i.e. at low intensity winds, which allows these delicate

24 structures to grow without breaking apart, and on very thin ice where a strong

25 temperature gradient is present between the ice surface and the overlying air

26 (Rankin et al., 2000; Rankin and Wolff, 2002 and references therein). Thus, frost

27 flowers formed at temperatures below -8 °C will be depleted in sodium and sulfate

28 relative to other ions present in seawater (Rankin et al., 2000; Rankin and Wolff,

29 2002), evidenced by negative $nssSO_4^{2-}$ values measured in aerosols and snow (see

30 section 2.3 for more details on the calculation of the nss-fractions).

1   For most of the last decade, frost flower formation, transport and deposition, has
2   been considered the most plausible mechanism behind the fractionated aerosol
3   detected at coastal areas. However, Yang et al. (2008 and 2010), and Huang and
4   Jaeglé (2017) proposed an alternative mechanism: the origin of sea-salt aerosol
5   could be due to the sublimation of blowing salty snow. This salty snow could be a
6   result of frost flower formation, upward migration of brine within the snow (Massom
7   et al., 2001), or by the input of sea-spray from the open ocean or nearby leads or
8   polynyas (Dominé et al., 2004). Flooding of sea-ice under the weight of accumulated
9   snow can also induce increased salinity of snow (Massom et al., 2001). As the snow
10 can be contaminated or wetted with fractionated brine or frost flowers, it could be
11 expected that this salty snow also shows such fractionation. As pointed by Yang et
12 al. (2008 and 2010), this salty snow can be transported by wind and if the air is not
13 saturated, the snow particles may lose water by sublimation and become sea-salt
14 aerosols. These aerosols could then be transported and deposited either by dry or
15 wet deposition, depending on local meteorology.
16 According to Abram et al. (2013), the idea proposed by Yang et al. (2008) is
17 plausible for coastal sites, along with the frost flower mechanism. Consequently,
18 snow present on new sea-ice and frost flowers are important features that,
19 combined with wind transport, need to be taken into account when interpreting the
20 sea-salt record of coastal ice and firn cores.
21 This study discusses sub-annual and long-term temporal changes in sea-salt and
22 major ion concentration measured in three recently drilled firn cores from different
23 ice rises located at Fimbul Ice Shelf (FIS): Kupol Ciolkovskogo, Kupol Moskovskij,
24 and Blåskimen Island, a 100 m long core drilled near the FIS edge (S100), and five
25 snow pits sampled along the ice shelf (Figure 1). The main goals of the present
26 study are to investigate possible mechanisms behind deposition, subannual, and
27 spatial variability of sea-salts in this coastal region. The results presented here
28 contribute to bridging the data gap existent at coastal Antarctic sites, and to the
29 improvement of current Antarctic sea-ice reconstructions based on sea-salt
30 chemical proxies.

2 Methods

2.1 Study area

With an extent of approximately $36\,500$ km^2, FIS is the largest ice shelf in the Haakon VII Sea (Figure 1). Fed by Jutulstraumen, the largest outlet glacier in DML, FIS is divided into a fast moving ice tongue, Trolltunga, directly feeding the central part of the ice stream, and slower surrounding parts. Several ice rises are found at FIS, varying in size from 15 to 1200 km^2, and located approximately 200 km apart. Early investigations in this area began during the International Geophysical Year (IGY) 1956/57 (Swithinbank, 1957; Lunde, 1961; Neethling, 1970) and continued during the last decades with focus on surface mass balance (SMB) variability in space and time (Melvold et al., 1998; Melvold, 1999; Rolstad et al., 2000; Isaksson and Melvold, 2002; Kaczmarska et al., 2004; Kaczmarska et al., 2006; Divine et al., 2009; Sinisalo et al., 2013; Schlosser et al., 2012, 2014; Langley et al., 2014; Vega et al., 2016). However, studies on spatial and temporal variability of chemical composition of snow and ice from this area are limited to water stable isotopes interpretations (Kaczmarska et al., 2004; Schlosser et al., 2012, 2014; Vega et al., 2016).

SMB obtained from the S100 core (Figure 1) retrieved at FIS shows a mean long-term accumulation rate of 0.3 m water equivalent per year (m w.e. yr^{-1}) for the period 1737–2000, with a significant negative trend in SMB for the period 1920–2000 (Kaczmarska et al., 2004). This negative trend in SMB has been reported in several shorter firn cores from the region (Isaksson and Melvold, 2002; Divine et al., 2009; Schlosser et al, 2014), including one record from the Kupol Ciolkovskogo ice rise (Vega et al., 2016).

More detailed information on previous campaigns, glaciological and meteorological conditions at FIS and the core sites at the ice rises, can be found in Vega et al. (2016) and Goel et al., (2017), and references therein, whereas an overview on Antarctic ice rises is given in Matsuoka et al. (2015).

2.2 Sampling

Three shallow firn cores were retrieved at different ice rises (Kupol Ciolkovskogo (KC), Kupol Moskovskij (KM), and Blåskimen Island (BI), Figure 1, Table 1), located

6

1   at FIS between January 2012 and January 2014 during field expeditions organized

2   by the Norwegian Polar Institute (NPI). Location, elevation, and length of the

3   different ice rises cores are presented in Table 1. Each core was drilled from the

4   bottom of a 2 m snow pit (not sampled for major ions). The firn density was

5   determined as bulk density of each sub-core piece (average length of 45 cm), and

6   of each snow pit interval (20 cm). The samples were collected following clean

7   protocols (Twickler and Whitlow, 1997), shipped frozen to NPI, and later to the Paul

8   Scherrer Institute (PSI), Switzerland, for cutting and chemical analysis. Sample

9   length varied between 4 and 8 cm depending on sample depth and density.

10 Thickness of ice lenses, water stable isotope ratios and SMB for the three ice rises

11 are reported in Vega et al. (2016). Additionally, unpublished major ion

12 concentrations measured in the 100 m deep S100 core drilled in austral summer

13 2000/2001 (Kaczmarska et al., 2004) were included in this study (Figure 1, Table 1).

14 In addition to the firn and ice cores, five snow pits (M1, M2, G3, G4, and G5, with

15 additional re-sampling of G4 and G5 as G4a and G5a) were sampled at different

16 sites at FIS during Nov.–Dec. 2009 by a field team from NPI (Figure 1, Table 1). The

17 snow pits were sampled at 20 cm (M1, M2, and G3, G4, and G5) and 4 cm (G4a

18 and G5a) intervals; samples were transported and kept frozen until analysis. The

19 previous summer surface at the snow pit sites was estimated to be located at a

20 depth between 120 and 160 cm (Sinisalo et al., 2013).

21 **2.3 Chemical analyses**

22 Major ions (methanesulfonic acid (MSA), Cl^-, NO_3^-, SO_4^{2-}, Na^+, K^+, Mg^{2+} and Ca^{2+})

23 present in the three firn cores from the ice rises were analysed at PSI using a

24 Metrohm ProfIC 850 ion chromatograph combined with an 872 Extension Module

25 and auto-sampler. The precision of the method was within 5 % and detection limits

26 (D.L.) were below 0.02 μmol L^{-1} for each ion (Wendl et al., 2014). Ion concentrations

27 (MSA, Cl^-, NO_3^-, SO_4^{2-}, Na^+, K^+, Mg^{2+} and Ca^{2+}) in the S100 core were measured at

28 the British Antarctic Survey (BAS) using fast ion chromatography (Littot et al., 2002).

29 The reproducibility of the measurements was 4–10 %.

The Cryosphere
Discussions

1   In addition, major ions (Cl^-, Br^-, NO_3^-, SO_4^{2-}, Na^+, K^+, Mg^{2+} and Ca^{2+}) were measured

2   in the FIS snow pits. Triplicate snow samples were taken at each depth interval.

3   Hence, average concentrations of each ion at each depth interval are reported here.

4   Additionally, pits G4 and G5 were sampled at 2 cm intervals, with one sample per

5   depth interval (pits G4a and G5a). For these snow pits sampled at high resolution

6   only Cl^-, NO_3^-, and SO_4^{2-} are available. All snow pit samples were transported frozen

7   from the sampling site to NPI and then to the Department of Earth Sciences,

8   Uppsala University, where major ions were quantified using a Metrohm ProfIC 850

9   ion chromatograph. The reproducibility of the measurements was within 5 % and

10   detection limits (DL) were below 0.3 $\mu mol\ L^{-1}$ for each ion.

11   Hereafter, brackets are used to denote ionic concentrations expressed in $\mu mol\ L^{-1}$.

12   Non sea-salt fractions were calculated from the mean seawater composition using

13   Na^+ as standard ion, using:

14   $$[\mathrm{nss}X] = [X]_{\mathrm{total}} - k \times [Na^+]_{\mathrm{total}},$$

15   where

16   $$k = \frac{[X]_{\mathrm{seawater}}}{[Na^+]_{\mathrm{seawater}}},$$

17   using the standard mean chemical composition of seawater with ion concentration

18   expressed in $\mu mol\ L^{-1}$.

19   In addition, water stable isotopes analyses of the KC, KM and BI cores are described

20   in Vega et al. (2016); while analysis of the S100 core is described in (Kaczmarska

21   et al., 2004). Water stable isotope analyses were not performed in the FIS snow

22   pits.

2.4   Firn and ice core timescales

24   The timescales of the KM and BI cores were obtained based on annual layer

25   counting of water stable isotope ratios ($\delta^{18}O$), and found to cover the periods

26   between austral winter-1995(96) and summer-2014, respectively. The error in the

27   dating was estimated as ± 1 year for both of these cores (Vega et al., 2016). Both

28   KC and the S100 cores were dated using a combination of annual layer counting of

29   $\delta^{18}O$ and identification of volcanic horizons (i.e. by using the SO_4^{2-}, dielectric profiling

30   (DEP), and electrical conductivity measurements (ECM)), with timescales covering

1 the time period 1958–2012 (± 3 years) at KC (Vega et al., 2016), and 1737–2000

2 (± 3 years) at S100 (Kaczmarska et al., 2004).

3 **2.5 Snow pits timescales**

4 Snow pits were dated by visually identifying the summer layer previous to the

5 digging, since no water stable isotope data were available. Consequently, a highly

6 precise dating (e.g. with monthly resolution) of the snow layers was not possible.

7 The previous summer layer in pits M1, M2 and G3–G5 was identified at 120–160 cm

8 depth according to Sinisalo et al. (2013); however, chemical sampling was done just

9 down to a depth of 60–90 cm in each snow pit reported in this study. Consequently,

10 the snow depth at the different snow pit sites in which ions were analysed represents

11 less than a year of accumulation (Table 1). The snow accumulation between top

12 and bottom in each snow pit agree with previously documented values estimated

13 for the most recent years at the different pit sites (Schlosser et al., 2014), being

14 slightly below the average annual accumulation, with the exception of pit G3, which

15 showed a higher accumulation between 0–90 cm depth than the average

16 accumulation rate at the site for the period 1993–2009 (Schlosser et al., 2014).

17 **3 Results**

18 **3.1 Ion concentrations and sources**

19 Median concentration values for all ions measured in the cores and snow pits are

20 shown in Table 2. In general, concentrations in the KM core are higher than in the

21 other ice rises cores, and snow pits, e.g. about eight-fold higher concentrations of

22 Na^+, K^+, Mg^{2+} and Cl^- in KM than in the KC core are found for the period 1995–2012.

23 The relatively high Na^+ and Cl^- concentrations observed in the KM core are also

24 detected in the upper meters of the S100 core (in the periods 1995–2000, and 1950–

25 2000, respectively, Table 2). Similarly high values have been reported in several

26 snow and firn samples from other western DML coastal sites (Kärkäs et al., 2005),

27 and in Mill Island, Wilkes Land (Inoue et al., 2017).

28 Ion concentrations in the snow pits are in reasonable agreement with firn and ice

29 core values reported in Table 2 and with ion concentration ranges for snow pits

1 previously sampled at FIS (Mulvaney et al., 1993). Temporal and spatial variability

2 of ion concentrations are explored in more detail in the following sections.

3 In order to assess the most important sources explaining the total variance in the

4 glacio-chemical records from FIS, a principal component analysis (PCA) was

5 applied to the different ion series measured at the KC, KM, BI, and S100 cores.

6 Years, in which no sub-annual concentrations were available in the S100 (1793,

7 1841, 1866, 1918, and 1944) due to low resolution, were filled in by linearly

8 interpolating between the annual means of the previous and following year. For the

9 PCA analysis, ion concentrations were logarithmized (at sub-annual (using the raw

10 values as input) and annual resolutions) and standardized by subtracting the mean

11 of the data series from each data point and then dividing the result by the standard

12 deviation of the data series. Due to the sampling resolution, only the KM and BI

13 cores were comparable at a sub-annual level. PCA analyses were performed for

14 three different periods of the S100 core: for the entire time interval spanning 1737–

15 2000, for the subsection between 1737–1949, and between 1950–2000.

16 The sum of the variances of the first three principal components (PC1, PC2 and

17 PC3) was ≥ 80 % of the total variance of the original sub-annual and annual data in

18 all cores. Since the results of the sub-annual and annual PCA analysis are similar

19 only the annual results are considered. The loadings of the first three (KC) and two

20 (KM, BI, and S100) principal components are shown in Table 3. PCA results are

21 consistent between the different cores. Consequently, the ions can be separated in

22 two main groups: sea-salts species (Na^+, Cl^-, K^+, Mg^{2+}, and Ca^{2+}) and marine-

23 biogenic/mixed (MSA, SO_4^{2-}, including NO_3^-) (Table 3).

24 Generally, our results indicate that the major sources of the ions at the different sites

25 are the same, independent of the core site and mean concentrations of ions in the

26 cores. Only at the KC site the PCA results imply an additional input of Ca^{2+} from

27 other sources than sea-salt, as for instance mineral dust. The high loadings of NO_3^-

28 and MSA in PC2, and thus, coherence between both species, was already observed

29 in an ice core from Lomonosovfonna, Svalbard (Wendl et al., 2015), and a fertilizing

30 effect was proposed as explanation. Enhanced atmospheric NO_3^- concentrations

31 and the corresponding nitrogen input to the ocean can trigger the growth of dimethyl-

1   sulfide-(DMS)-producing phytoplankton. However, there is a variety of possible NO_3^-

2   sources and the relative importance of these sources at certain locations and time

3   is still in discussion (Mulvaney and Wolff, 1993; Savarino et al., 2007; Wolff et al.

4   2008; Weller et al. 2011; Pasteris et al., 2014; Sofen et al. 2014).

5   **3.2   Long-term variability of ion concentrations**

6   We use the two longest available records for FIS (KC and S100) to explore the long-

7   term temporal variability of major ions, with special focus on sea-salts, represented

8   by Cl^- and Na^+ (Figure 2). In the S100 core, Na^+, Cl^-, K^+, SO_4^{2-}, Mg^{2+}, and Ca^{2+}

9   concentrations show a marked six-fold increase after the 1950s. However, there is

10   no significant increase of the concentration of these species in the KC core. Due to

11   its limited time coverage it cannot be determined if there was a substantial relative

12   increase in concentrations at this site after the 1950s. MSA and NO_3^- concentrations

13   do not show such marked increase in the S100 core and values agree between both

14   cores after the 1950s (Figure S1 in the supplementary material). Consequently,

15   three periods can be distinguished in the S100 record: (i) the period between 1995–

16   2000, comparable to the time covered by the KM and BI cores; (ii) the period

17   between 1737–1949, where ion concentrations remain low; and, (iii) the period

18   between 1950–2000, where sea-salt concentrations increased (Table 2).

19   With the exception of MSA, all ions show a positive trend (significant at the 95 %

20   confidence level) during the 1950–2000, although the slope for NO_3^- is three orders

21   of magnitude smaller than for the other ions (slope and error of the linear regression

22   are shown in Table S1 in the supplementary material). Such a linear trend was not

23   observed in the ion records from the KC core over the same period.

24   Ions, with the exception of MSA, also show a positive and significant trend between

25   1737–1949, (Table S1), however, the increase is less marked than during 1950–

26   2000 period.

27   **3.3   Sub-annual variability of ion concentrations**

28   To investigate the seasonality of the different ion groups in the KM, BI, and S100

29   cores, a composite year of data was produced for each ion species, i.e. for each

1   year, a linear interpolation was done in the concentration domain of each ion at a

2   resolution of 0.01-years (3.65 days). The seasonal concentration averages were

3   then calculated for the months MAM (autumn), JJA (winter), SON (spring) and DJF

4   (summer). All ion concentrations were expressed in μmol L^{-1} and were

5   logarithmized. Ion concentrations were not available at the top 2 m (snow pit data),

6   therefore, the composite year consisted of 16 (1996–2011) and 15 (1997–2011)

7   complete years for the KM and BI cores, respectively. In the S100 core,

8   seasonalities were investigated only during the period 1995–2000, where the

9   concentrations have sufficient temporal resolution for subannual analyses. The

10   resulting seasonal average concentrations in the cores are presented in Figure 3.

11   Sea-salt species (Na$^+$ and Cl$^-$, Figure 3a) show minimum concentrations during

12   spring in the KM core, whereas in the S100 core minimum values are reached during

13   summer. Maximum concentrations are reached during summer (KM) and

14   spring/autumn (S100). In the BI core, sea-salt seasonalities are less pronounced.

15   Both Mg^{2+} and Ca^{2+} (Figure 3b) show high values in summer in the KM core, and in

16   spring in the S100 core, whereas, again, a less marked seasonality is observed in

17   the BI core. MSA concentrations (Figure 3c) show consistent and marked

18   spring/summer maxima in all three cores, and a marked winter minima in the BI

19   core, which is in agreement with the main source of MSA (marine-biogenic) most

20   active during the warmer months. The MSA winter minimum is not as pronounced

21   in the KM core as in the BI core, while the MSA minimum is reached in autumn in

22   the S100 core. NO$_3^-$ and SO$_4^{2-}$ concentrations (Figure 3d) show a distinct increase

23   toward the spring/summer in the BI core, which is also observed in the KM core,

24   although less defined. In the S100 core, higher NO$_3^-$ and SO$_4^2$ concentrations are

25   found during the spring.

26   **3.4 Ions spatial variability**

27   In order to investigate ion spatial variability at FIS, we used median ion

28   concentrations in the different snow pits (M1, M2, G3, G4, and G5), and ice rises

29   cores (KM and BI) for the year 2009, and compared them with latitude, longitude,

30   and distance from the sea (Table 4). Since it has been found that the chemical

The Cryosphere
Discussions

Open Access

EGU

1 records in the KM and BI cores appear to be affected by surface topography and

2 local meteorological conditions (Vega et al., 2016), we also calculated the

3 correlation coefficients (R values) between concentration and latitude, longitude,

4 and distance from the sea, only using the snow pit data.

5 Concentrations of Br^-, Na^+, K^+, Mg^{2+} and Ca^{2+} show a significant decrease at the

6 95 % confidence level with increased latitude, i.e. with increasing distance from the

7 coast. Correlation coefficients are high for Cl^- and SO_4^{2-}, however, not significant.

8 No significant relationship is found between the median ion concentrations and

9 longitude for any of the species. When comparing concentrations with the distance

10 from the sea (obtained from the GIS package Quantarctica, www.quantarctica.org),

11 it was found that Br^-, SO_4^{2-}, Na^+, and Ca^{2+} show a significant decrease with

12 increasing distance from the sea when only the snow pits are considered in the

13 analysis; i.e. significance is lost when the KM and BI 2009 median values are

14 included. These findings agree with previous studies from western Dronning Maud

15 Land (WDML) (Stenberg et al., 1998), confirming that sea-salt concentrations are

16 strongly dependent on the distance from the sea in this area. This relationship loses

17 significance when the records from the ice rises KM and BI are included, reflecting

18 the influence of local effects on annual SMB at these sites (Vega et al., 2016).

19 Since the elevation differences between the snow pits are only in the order of tens

20 of meters, we did not investigate the elevation dependence of mean ion

21 concentrations.

22 **3.5 Deposition regimes**

23 In order to explain the marked increase in ion concentrations after the 1950s, and

24 the negative trend observed in SMB for the S100 and KC cores for the second half

25 of the 20th century (Figure 2e and f) (Vega et al., 2016), we investigated the

26 deposition regimes at FIS. We employed correlation analysis to assess the

27 relationship between the annual average concentrations of all ions and annual SMB

28 at the different core sites for the respective period covered by each core (as noted

29 in Table 2). Correlation coefficients (R_{conc}, Table 5) were < 0.57 and non-significant

30 at the 95 % confidence interval (with the exception of NO_3^- and SO_4^{2-} in the S100

1 core), which indicates that accumulation rates, and thus, wet deposition is not

2 controlling the ion concentration at the different core sites at FIS. We also

3 investigated the relationship between chemical flux, expressed as μmol cm^{-2} yr^{-1}

4 and annual snow accumulation at the different core sites (R_{flux}, Table 5). A

5 significant positive correlation between fluxes and accumulation exists for almost all

6 ion species analysed in the different cores with the exception of sea-salts in the

7 S100 core, with significant R_{flux} values larger than 0.5 for most ions (with the

8 exception of MSA in the KC and S100 cores, and SO_4^{2-}, Mg^{2+} and Ca^{2+} in the S100

9 core). This indicates that most of the variance in the ion flux can be explained by

10 changing snow accumulation rate at each site for most of ions, with the exception

11 of sea-salts in the S100 core. Therefore, dry deposition of sea-salt aerosols would

12 be the controlling factor in sea-salt fluxes at the S100 site. To confirm that the

13 increase in sea-salt fluxes observed after the 1950s is due to a change in sea-salt

14 deposition mechanism, we calculated the R_{conc} and R_{flux} values for the periods

15 1737–1949 and 1950–2000 (Table 5). While R_{conc} values for both periods were not

16 significant and low, during 1737–1949, all R_{flux} values were significant (R>0.41). This

17 indicates that during the period 1737–1949, most of the variance in all ion fluxes can

18 be related to SMB at the S100 site. Sea-salt R_{flux} values decreased (with the

19 exception of R_{flux} of NO_3^-) and became non-significant in the case of Cl^-, SO_4^{2-}, and

20 Ca^{2+} during the 1950–2000 period, which points to a change in the deposition

21 regime after the 1950s.

22 **3.6 Evidence for increased fractionated nss-SO_4^{2-} after 1950s**

23 In order to evaluate the possible effect of fractionated aerosols as a source of sea-

24 salts to the snow on FIS, we calculated the nssSO_4^{2-} fraction as described in section

25 2.3, using *k* values of 0.06 (see supplementary material in Vega et al., 2015). The

26 percentage of nssSO_4^{2-} relative to total SO_4^{2-} is two- to three-times higher in the KC

27 core than in the other ice rises cores, KM and BI. Negative median nssSO_4^{2-} values

28 were obtained in the S100 core and snow pits M1, M2, G3, and G4. These negative

29 values, i.e. nssSO_4^{2-} is strongly depleted in SO_4^{2-} relative to Na^+ (Rankin and Wolff,

30 2002), suggest a possible role of frost flowers and wind-blown salty snow as source

1   of sea-salts to the S100 core (Figure 4a y b, black line). We therefore followed the

2   approach by Inoue et al. (2017), to obtain a new value of k, k'. This k' was calculated

3   by subtracting the slope of the linear regression (slope= 0.02, in Figure 5) for the

4   nssSO$_4^{2-}$ concentrations vs. Na$^+$ concentrations (for the whole period, i.e. 1737–

5   2000) from the constant k (calculated as described in section 2.3), i.e. k'= 0.04 (in

6   μmol L^{-1}). Similarly, we calculated k'' for the period 1737–1949 (k''=0.02), and k''' for

7   the period 1950–2000 (k'''= k'=0.04). The nssSO$_4^{2-}$ fraction without the effect of

8   sulfate fractionation was recalculated using the values of k', and k'' (Table 6, and

9   Figure 4a y b, red and blue lines). nssSO$_4^{2-}$ for the KC, KM, and BI cores is shown

10   in Figure 4c (calculated using k=0.06). The k' value recalculated for the S100 core

11   is similar to the k' values described by Palmer et al. (2002), and Plummer et al.

12   (2012) at Law Dome, while k'' is similar to the value obtained by Inoue et al. (2017)

13   for a Mill Island coastal core. Negative nssSO$_4^{2-}$ values are more pronounced after

14   the 1950s, which will be discussed in the following sections.

15   **4   Discussion**

16   From the spatial and temporal variability of sea-salt concentrations in the different

17   FIS cores and snow pits discussed here, it seems that more than one mechanism

18   is contributing to the load of sea-salts at FIS, in agreement with the findings by

19   Abram et al. (2013). The ice core data from S100 also suggest that there was a

20   change in sea-salt deposition regime after the 1950s evidenced by an increase, up

21   to six-fold, of median sea-salt concentrations after the 1950s in comparison with the

22   previous 200 years. This increase in concentration is accompanied by a clear shift

23   in nssSO$_4^{2-}$ toward negative values, indicative of SO$_4^{2-}$ fractionation in sea-salts.

24   The negative nssSO$_4^{2-}$ values found in the FIS records could be explained by an

25   enhanced input of sea-salt from (i) windblown frost flowers and/or (ii) aerosol formed

26   after fractionated salty-snow sublimation, with both (i) and (ii) being formed in the

27   neighbouring waters at the eastern flank of FIS. Yang et al. (2008) have reported

28   that aerosol production via (ii) can be more than one-fold larger per unit area than

29   sea-salt production from the open ocean. There is no or very limited amount of multi-

30   annual sea-ice near FIS, and young sea-ice formed during winter in the vicinity of

1   the S100 site is quickly covered by snow due to cyclonic activity. Trajectory studies

2   of air with high sea-salts concentrations and low sulfate/sodium ratios arriving at

3   Halley station, showed that these air masses mainly originate at regions where

4   young sea-ice and frost flowers are formed (Hall and Wolff, 1998; Rankin and Wolff,

5   2002). However, conditions at Halley are not comparable to FIS, since the main

6   easterly or north-northeasterly wind direction prevailing at Halley means an off-land

7   air flow, thus creation of polynyas with open water and consecutive new ice

8   formation, whereas at FIS, and most of the Dronning Maud Land coast, the wind is

9   mainly parallel to the coast or even slightly towards the coast. In particular, a

10 quantification of the areas covered by frost flowers is still missing. It is possible that

11 those areas are comparatively small due to the generally high wind speeds

12 prevailing above the Southern Ocean, resulting in a high percentage of frazil ice,

13 and synoptic conditions lead to the quick development of a snow cover on the young

14 sea-ice. Although it is not possible to apportion the contribution of fractionated sea-

15 salts via (i) or (ii) with the current data, it is plausible that a larger contribution of

16 fractionated aerosol formed from salty-snow than by frost flowers, in agreement with

17 dry deposition of sea-salts as pointed in section 3.5. In addition, frequent stormy

18 conditions in the area are detrimental for the formation of frost flowers, which form

19 under quiet, undisturbed conditions, usually only in leads or small polynyas under

20 the influence of anticyclonic weather. This also means low wind speeds and thus

21 not much transport of frost flowers to the sampling sites at FIS. Thus, mechanism

22 (ii), blowing salty snow formed on thin sea-ice that sublimates during transport to

23 form sea-salt aerosols, appears as a much more probable explanation considering

24 the local meteorological conditions in the study area.

25 Considering the dominant wind direction at FIS (ENE), and the size of frost flowers

26 (10–20 mm) and aerosol formed via (ii) (size >0.95 μm) (Seguin et al., 2014), wind

27 transport would be more efficient from the neighbouring waters to the low elevation

28 sites (e.g. S100 and the snow pit sites) than to the more elevated ice rises sites.

29 This hypothesis is reinforced by the fact that negative $nssSO_4^{2-}$ values are mostly

30 registered in the low elevation sites S100, M1, M2, G3, and G4, but not in the more

31 elevated ice rises sites KC, KM, and BI, where the median $nssSO_4^{2-}$ values for the

1   cores are all positive, and sea-salt concentrations considerably lower than at S100

2   (with the exception of KM, which will be discussed below).

3   The dramatic increase in fractionated sea-salt in the S100 core after 1950s could

4   be associated with an enhanced production of fractionated aerosol and frost flowers

5   in the waters at the eastern flank of FIS as a response to the calving of ice at the tip

6   of FIS (Figure 1), which occurred in 1967 (Vinje, 1975). The longer Trolltunga

7   present before the calving event could have formed a larger bay to the east of it,

8   where compaction of the sea ice occurred due to prevailing easterly winds, resulting

9   in thicker, longer-lasting sea-ice, which limited the sea-spray formation. Such thick

10 sea-ice does not form under post-calving event conditions, e.g. with a shorter

11 tongue. Post-calving event conditions would mean that more sea-spray could be

12 formed and deposited at the FIS sites compared with pre-calving periods. However,

13 sea-spray enhancing alone cannot account for either the increase of sea-salt

14 concentrations or the negative $nssSO_4^{2-}$ found in snow and ice samples. In order to

15 explain the fractionated sea-salt values detected in the S100 cores, there must be

16 an enhanced source of fractionated sea-salts after the calving event. This would be

17 the case if young sea-ice (where fractionation of sea-salts can take place) formed

18 nearby the S100 site as a result of the greater area of open sea available after the

19 calving event. This hypothesis could be tested by closer analysis of satellite and

20 historical sea-ice data, which, however, is beyond the scope of the present study.

21 Other possible mechanisms, such as deposition of sea salts with rime or windblown

22 snow present over multi-annual sea ice, can explain neither the increase in sea salt

23 concentration nor the fractionation observed in S100 after the 1950s. Additionally,

24 annual averages of monthly zonal and meridional wind speeds (ERA40, Uppala et

25 al., 2005) for the area (69°S–71°S, 3.5°W–5°E) between 1955–2001 (Figure 6)

26 show no significant positive trends, thus evidencing that the S100 sea-salt increase

27 after 1950s cannot be related to enhanced transport by wind.

28 Due to the limited time coverage of the KC, KM, and BI cores, we do not know

29 whether there was a relative increase in sea-salt concentrations in the ice rises

30 cores after the 1950s. There is no signal of fractionated sea-salts in any of the ice

31 rises cores (e.g. no significant negative $nssSO_4^{2-}$ values), which suggests that the

1 main source of sea-salts at these sites is wet deposition of sea-spray. Relatively

2 higher sea-salt concentrations measured in the KM core in comparison to the other

3 ice rises cores could be explained by a combination of distance to the sea and the

4 prevailing precipitation and wind conditions in the area: precipitation on FIS is mainly

5 caused by frontal systems of cyclones in the circumpolar trough that move

6 eastwards north of the coast, thus leading to easterly or east-north-easterly surface

7 winds on FIS (Schlosser et al., 2008). This means that even though BI is equally

8 close to the sea as KM (Figure 1), KM has by far the shortest distance to the source

9 of marine aerosols of all three cores, which could explain the comparatively high

10 sea-salt concentrations (Table 1).

11 **5   Conclusions**

12 This study reports subannual and long-term temporal sea-salt and major ion

13 concentration changes measured in three recently drilled firn cores from different

14 ice rises located at Fimbul Ice Shelf (FIS): Kupol Ciolkovskogo, Kupol Moskovskij,

15 and Blåskimen Island, a 100 m long core drilled near the FIS edge (S100), and five

16 snow pits sampled along the ice shelf. We found that Na^+ concentrations decrease

17 with latitude and distance from the sea when low elevation sites are considered

18 (S100 and the FIS snow pits). A significant increase in sea-salts is observed in the

19 S100 core after the 1950s, which is associated with a change in sea-salt sources.

20 This increase in sea-salt concentrations was accompanied by a shift in $nssSO_4^{2-}$

21 toward negative values, suggesting the input of fractionated sea-salts to the ion load

22 in the S100 core most likely by dry deposition. Such dry deposition regime is not

23 observed in any of the ice rises cores, and evidence of a significant contribution of

24 fractionated sea-salt aerosols to these sites was not found. Consequently, the

25 results of this study suggest that the S100 record contains a more local sea-salt

26 signal, dominated by processes during sea-ice formation in the neighbouring waters,

27 whereas the ice rises cores record the signal of larger-scale conditions of

28 atmospheric flow and transport of sea-salt aerosols produced over open water.

29 These findings are of vital importance for the understanding of the mechanisms of

30 sea-salt aerosol production, transport and deposition at coastal Antarctic sites, and

1 for the improvement of the current Antarctic sea-ice reconstructions based on sea-

2 salt chemical proxies.

6 Data availability

4 For the chemistry profiles of the KC, KM, BI, and S100 cores, and FIS snow pits,

5 please contact E. Isaksson (elisabeth.isaksson@npolar.no).

6 ERA40 reanalysis data is available at https://climatedataguide.ucar.edu/climate-

7 data/era40 (Uppala, et al., 2005).

8

1 **References**

2 Abram, N. J., Wolff, E. W., and Curran, M. A. J.: A review of sea ice proxy information

3 from polar ice cores, Quat. Sci. Rev., 79, doi:10.1016/j.quascirev.2013.01.011,

4 2013.

5 Curran, M., van Ommen, T., and Morgan, V.: Seasonal characteristics of the major

6 ions in the high-accumulation dome Summit South ice core, Law Dome, Antarctica,

7 Ann. Glaciol., 27, 385–390, 1998.

8 Divine, D.V., Isaksson, E., Kaczmarska, M., Godtliebsen, F., Oerter, H., Schlosser,

9 E., Johnsen, S.J., van den Broeke, M. and van de Wal, R.S.W.: Tropical Pacific -

10 High Latitude South Atlantic Teleconnections as Seen in the $\delta^{18}O$ Variability in

11 Antarctic Coastal Ice Cores, J. Geophys. Res., 114, D11112,

12 doi:10.1029/2008JD010475, 2009.

13 Fischer, H., Siggaard-Andersen, M. -L., Ruth, U., Röthlisberger, R., and Wolff, E.:

14 Glacial/interglacial changes in mineral dust and sea-salt records in polar ice cores:

15 Sources, transport and deposition, Rev. Geophys., 45, RG1002,

16 doi:10.1029/2005RG000192, 2007.

17 Goel, V. Brown, and J. Matsuoka, K. Glaciological Settings and recent mass balance

18 of the Blåskimen Island in Dronning Maud Land, Antarctica. The Cryosphere

19 Discuss., https://doi.org/10.5194/tc-2017-61, 2017.

20 Hall, J.S., and Wolff, E.W.: Causes of seasonal and daily variations in aerosol

21 seasalt concentrations at a coastal Antarctic station. Atmospheric Environment, 32

22 (21), 3669e3677. http://dx.doi.org/10.1016/s1352-2310(98)00090-9, 1998.

23 Huang, J., and Jaeglé, L.: Wintertime enhancements of sea salt aerosol in polar

24 rigions consistent with a sea ice source from blowing snow, Atmos. Chem. Phys.,

25 17, 3699–3712, doi:10.5194/acp-17-3699-2017, 2017.

26 Inoue, M., Curran, M. A. J., Moy, A. D., van Ommen, T. D., Fraser, A. D., Phillips,

27 H. E., and Goodwin, I. D.: A glaciochemical study of 120 m ice core from Mill Island,

28 East Antarctica, Clim. Past, 13, 437-453, doi:10.5194/cp-13-437-2017, 2017.

29 Isaksson, E. and Melvold, K.: Trends and patterns in the recent accumulation and

30 oxygen isotopes in coastal Dronning Maud Land, Antarctica: interpretations from

31 shallow ice cores, Ann. Glaciol., 35, 175–180, 2002.

1   Jourdain, B., S. Preunkert, O. Cerri, H. Castebrunet, R. Udisti, and Legrand, M.:

2   Year-round record of size-segregated aerosol composition in central Antarctica

3   (Concordia station): Implications for the degree of fractionation of sea-salt particles,

4   J. Geophys. Res., 113, D14308, doi:10.1029/2007JD009584, 2008.

5   Kaczmarska, M., Isaksson, E., Karlöf, L., Winther, J-G., Kohler, J., Godtliebsen, F.,

6   Ringstad Olsen, L., Hofstede, C. M., Van Den Broeke, M. R., Van De Wal, R. S.W.,

7   Gundestrup, N.: Accumulation variability derived from an ice core from coastal

8   Dronning Maud Land, Antarctica, Ann. Glaciol. 39, 339–345, 2004.

9   Kaczmarska, M., Isaksson, E., Karlöf, L., Brandt, O., Winther, J-G., Van De Wal, R.,

10 Van Den Broeke, M. R., Johnsen, S.: Ice core melt features in relation to Antarctic

11 coastal climate, Antarc. Science, 18(2), 271–278, 2006.

12 Kreutz, K.J., Mayewski, P.A., Whitlow, S.I., and Twickler, M.S.: Limited migration of

13 soluble ionic species in a Siple Dome, Antarctica, ice core. In: Budd, W.F. (Ed.),

14 Ann. Glaciol., vol. 27, 371–377, 1998.

15 Kärkäs, E., Martma, T., and Sonninen, E.: Physical properties and stratigraphy of

16 surface snow in western Dronning Maud Land, Antarctica, Polar Res., 24(1–2), 55–

17 67, 2005.

18 Langley, K., Kohler, J., Sinisalo, A., Øyan, M. J., Hamran, S. E., Hattermann, T.,

19 Matsuoka, K., Nøst, O. A. and Isaksson E.: Low melt rates with seasonal variability

20 at the base of Fimbul Ice Shelf, East Antarctica, revealed by in situ interferometric

21 radar   measurements,   Geophys.   Res.   Lett.,   41,   8138–8146,

22 doi:10.1002/2014GL061782, 2014.

23 Levine, J. G., Yang, X., Jones, A. E., and Wolff, E. W.: Sea salt as an ice core proxy

24 for past sea ice extent: A process-based model study, J. Geophys. Res. Atmos.,

25 119, 5737–5756, doi:10.1002/2013JD020925, 2014.

26 Littot, G. C., Mulvaney, R., Röthlisberger, R., Udisti, R., Wolff, E. W., Castellano, E.,

27 De Angelis, M., Hansson, M. E., Sommer, S. and Steffensen, J. P.: Comparison of

28 analytical methods used for measuring major ions in the EPICA Dome C (Antarctica)

29 ice core, Ann. Glaciol., 35, 299–305, 2002.

1   Lunde, T.: On the snow accumulation in Dronning Maud Land. Den Norske

2   Antarktischspedisjonen 1956–60, Scientific Results No. 1. Norsk Polarinstitutt

3   Skrifter No. 123, 1961.

4   Massom, R.A., Eicken, H., Haas, C., Jeffries, M.O., Drinkwater, M.R., Sturm, M.,

5   Worby, A.P., Wu, X.R., Lytle, V.I., Ushio, S., Morris, K., Reid, P.A., Warren, S.G.,

6   Allison, I.: Snow on Antarctic sea ice, Rev. Geophys., 39 (3), 413-445.

7   http://dx.doi.org/10.1029/2000rg000085, 2001.

8   Matsuoka, K., Hindmarsh, R. C. A., Moholdt, G., Bentley, M. J., Pritchard, H. D.,

9   Brown, J., Conway, H., Drews, R., Durand, G., Goldberg, D., Hattermann, T.,

10 Kingslake, J., Lenaerts, J. T. M., Martín, C., Mulvaney, R., Nicholls, K., Pattyn, F.,

11 Ross, N., Scambos, T., and Whitehouse, P.: Antarctic ice rises and rumples: Their

12 properties and significance for ice-sheet dynamics and evolution, Earth-Sci. Rev.,

13 150, 724–745, 2015.

14 Melvold, K.: Impact of recent climate on glacier mass balance: studies on

15 Kongsvegen, Svalbard and Jutulstraumen, Antarctica, D.Sc. thesis, University of

16 Oslo., Department of Geography Report 13, 1999.

17 Melvold, K., Hagen, J. O., Pinglot, J. F. and Gundestrup, N.: Large spatial variation

18 in accumulation rate in Jutulstraumen ice stream, Dronning Maud Land, Antarctica,

19 Ann. Glaciol., 27, 231–238, 1998.

20 Mulvaney, R., Coulson, G. F. J. and Corr, H. F. J.: The fractionantion of sea salt and

21 acids during transport across an Antarctic ice shelf, Tellus, 45B, 179–187, 1993.

22 Mulvaney R., and Wolff, E. W.: Evidence for Winter/Spring Denitrification of the

23 Stratosphere in the Nitrate Record of Antarctic Firn Cores, J. Geophys. Res.,

24 98(D3), 5213–5220, 1993.

25 Neethling, D. C.: Snow accumulation on the Fimbul ice shelf, western Dronning

26 Maud Land, Antarctica, International Association of Scientific Hydrology Publication

27 86 (Symposium at Hanover1968—Antarctic Glaciological Exploration (ISAGE)),

28 390–404, 1970.

29 Palmer, A. S., Morgan, V. I., Curran, M. A. J., van Ommen, T. D., and Mayewski, P.

30 A.: Antarctic volcanic flux ratios from Law Dome ice cores, Ann. Glaciol., 35, 329–

31 332, doi:10.3189/172756402781816771, 2002.

22

The Cryosphere
Discussions

1 Pasteris, D. R., McConnell, J. R., Das, S. B., Criscitiello, A. S., Evans, M. J., Maselli,

2 O. J., Sigl, M., and Layman, L.: Seasonally resolved ice core records from West

3 Antarctica indicate a sea ice source of sea-salt aerosol and a biomass burning

4 source of ammonium, J. Geophys. Res. Atmos., 119, 9168–9182,

5 doi:10.1002/2013JD020720, 2014.

6 Paterson, W. S. B.: The Physics of Glaciers, 3rd Edn., Butterworth-Heinemann,

7 Birlington, 469 pp., 1994.

8 Petit J.R., Jouzel J., Raynaud D., Barkov N.I., Barnola J.M., Basile, I., Bender, M.,

9 Chappellaz, J., Davis, M., Delaygue, G., Delmotte, M., Kotlyakov, V. M., Legrand,

10 M., Lipenkov, V. Y., Lorius, C., Pépin, L., Ritz, C., Saltzman E., and Stievenard, M.:

11 Climate and Atmospheric History of the Past 420,000 years from the Vostok Ice

12 Core, Antarctica, Nature, 399, 429-436, 1999.

13 Philippe, M., Tison, J.-L., Fjøsne, K., Hubbard, B., Kjaer, H. A., Lenaerts, J. T. M.,

14 Drews, R., Sheldon, S. G., De Bondt, K., Claeys, P., and Pattyn, F.: Ice core

15 evidence for a 20th century increase in surface mass balance in coastal Dronning

16 Maud Land, East Antarctica, The Cryosphere, 10, 2501–2516, doi:10.5194/tc-10-

17 2501-2016, 2016.

18 Plummer, C. T., Curran, M. A. J., van Ommen, T. D., Rasmussen, S. O., Moy, A.

19 D., Vance, T. R., Clausen, H. B., Vinther, B. M., and Mayewski, P. A.: An

20 independently dated 2000-yr volcanic record from Law Dome, East Antarctica,

21 including a new perspective on the dating of the 1450s CE eruption of Kuwae,

22 Vanuatu, Clim. Past, 8, 1929–1940, doi:10.5194/cp-8-1929-2012, 2012.

23 Rankin, A. M., Auld, V., and Wolff, E. W.: Frost flowers as a source of fractionated

24 sea salt aerosol in the polar regions, Geophys. Res. Lett., 27(21), 3469–3472,

25 doi:10.1029/2000GL011771, 2000.

26 Rankin, A. M. and Wolff, E. W.: Frost flowers: Implications for tropospheric chemistry

27 and ice core interpretation, J. Geophys. Res., 107(D23), 4683,

28 doi:10.1029/2002JD002492, 2002.

29 Rankin, A.M., and, Wolff, E.W.: A year-long record of size-segregated aerosol

30 composition at Halley, Antarctica, J. Geophys. Res. Atmos., 108 (D24), 4775,

31 http://dx.doi.org/10.1029/2003jd003993, 2003.

1   Rankin, A. M., Wolff, E. W., and Mulvaney, R.: A reinterpretation of sea-salt records
2   in Greenland and Antarctic ice cores?, Ann. Glaciol., 39, 276–282,
3   doi:10.3189/172756404781814681, 2004.
4   Rolstad, C., Whillans, I. M., Hagen, J. O. and Isaksson, E.: Large-scale force budget
5   of an outlet glacier: Jutulstraumen, Dronning Maud Land, East Antarctica, Ann.
6   Glaciol., 30(1), 35–41, 2000.
7   Roscoe, H. K., Brooks, B., Jackson, A. V., Smith, M.H., Walker, S. J., Obbard, R.
8   W., and Wolff. E. W.: Frost flowers in the laboratory: Growth, characteristics,
9   aerosol, and the underlying sea ice, J. Geophys. Res., 116, D12301,
10 doi:10.1029/2010JD015144, 2011.
11 Savarino, J., Kaiser, J., Morin, S., Sigman, D., Thiemens, M.: Nitrogen and oxygen
12 isotopic constraints on the origin of atmospheric nitrate in coastal Antarctica, Atmos.
13 Chem. Phys., 7, 1925–1945, 2007.
14 Seguin, A. M., Norman, A.-L., and Barrie, L.: Evidence of sea ice source in aerosol
15 sulfate loading and size distribution in the Canadian High Arctic from isotopic
16 analysis, J. Geophys. Res. Atmos., 119 (2), 1087–1096,
17 doi:10.1002/2013JD020461, 2014.
18 Schlosser, E., Anschütz, H., Isaksson, I., Martma, T., Divine, D., and Nøst, O.-A.:
19 Surface mass balance and stable oxygen isotope ratios from shallow firn cores on
20 Fimbulisen, East Antarctica, Ann. Glaciol., 53, 70–78,
21 doi:10.3189/2012AoG60A102, 2012.
22 Schlosser, E., Anschütz, H., Divine, D., Martma, T., Sinisalo, A., Altnau, S., and
23 Isaksson, E., Recent climate tendencies on an East Antarctic ice shelf inferred from
24 a shallow firn core network, J. Geophys. Res. Atmos., 119, 6549–6562, 2014.
25 Schlosser, E., Duda, M. G., Powers, J. G., and Manning, K. H.: The precipitation
26 regime of Dronning Maud Land, Antarctica, derived from AMPS (Antarctic
27 Mesoscale Prediction System) Archive Data, J. Geophys. Res., 113, D24108,
28 doi:10.1029/2008JD009968, 2008.
29 Sinisalo, A., Anschütz, H., Aasen, A. T., Langley, K., von Deschwanden, A., Kohler,
30 J. Matsuoka, K., Hamran, S. E., Øyan, M. J., Schlosser, E., Hagen, J. O., Nøst, O.
31 A., and Isaksson, E.: Surface mass balance on Fimbul ice shelf, East Antarctica:

24

1   Comparison of field measurements and large-scale studies, J. Geophys. Res.

2   Atmos., 118, 11,625–11,635, doi:10.1002/jgrd.50875, 2013.

3   Sofen, E. D., Alexander, B., Steig, E. J., Thiemens, M. H., Kunasek, S. A., Amos,

4   H. M., Schauer, A. J., Hastings, M. G., Bautista, J., Jackson, T. L., Vogel, L. E.,

5   McConnell, J. R., Pasteris, D. R., and Saltzman, E. S.: WAIS Divide ice core

6   suggests sustained changes in the atmospheric formation pathways of sulfate and

7   nitrate since the 19th century in the extratropical Southern Hemisphere, Atmos.

8   Chem. Phys., 14, 5749–5769, 2014.

9   Stenberg, M., Isaksson, E., Hansson, M., Karlén, W., Myewski, P. A., Twickler, M.

10   S., Whitlow, S. I., and Gundestrup, N.: Spatial variability of snow chemistry in

11   western Dronning Maud Land, Antarctica, Ann. Glaciol., 27, 378–384, 1998.

12   Swithinbank, C.: Glaciology I: A, The morphology of the Ice Shelves of western

13   Dronning Maud Land; B, The Regime of the Ice Shelves at Maudheim as shown by

14   Stake Measurements. Norwegian-British-Swedish Antarctic Expedition, 1949–52.

15   Scientific Results, Vol. III, 1957.

16   Stenni, B., Curran, M. A. J., Abram, N. J., Orsi, A., Goursaud, S., Masson-Delmotte,

17   V., Neukom, R., Goosse, H., Divine, D., van Ommen, T., Steig, E. J., Dixon, D. A.,

18   Thomas, E. R., Bertler, N. A. N., Isaksson, E., Ekaykin, A., Frezzotti, M., and

19   Werner, M.: Antarctic climate variability at regional and continental scales over the

20   last 2,000 years, Clim. Past Discuss., doi:10.5194/cp-2017-40, in review, 2017.

21   Thomas, E. R., van Wessem, J. M., Roberts, J., Isaksson, E., Schlosser, E., Fudge,

22   T., Vallelonga, P., Medley, B., Lenaerts, J., Bertler, N., van den Broeke, M. R.,

23   Dixon, D. A., Frezzotti, M., Stenni, B., Curran, M., and Ekaykin, A. A.: Review of

24   regional Antarctic snow accumulation over the past 1000 years, Clim. Past Discuss.,

25   doi:10.5194/cp-2017-18, in review, 2017.

26   Twickler, M., and Whitlow, S. Appendix B, in: Guide for the collection and analysis

27   of ITASE snow and firn samples, edited by: Mayewski, PA., and Goodwin, I.D.,

28   International Trans-Antarctic Scientific Expedition (ITASE), Bern, Past Global

29   Changes (PAGES report 97-1), 1997.

30   Udisti, R., Dayan, U., Becagli, S., Busetto, M., Frosini, D., Legrand, M., Lucarelli, F.,

31   Preunkert, S., Severi, M., Traversi, R., and Vitale, V.:Sea spray aerosol in central

1   Antarctica. Present atmospheric behaviour and implications for paleoclimatic

2   reconstructions, Atmos. Environ., 52, 109–120, 2012.

3   Uppala, S. M., Kållberg, P. W., Simmons, A. J., Andrae, U., Da Costa Bechtold, V.,

4   Fiorino, M., Gibson, J. K., Haseler, J., Hernandez, A., Kelly, G. A., Li, X., Onogi, K.,

5   Saarinen, S., Sokka, N., Allan, R. P., Andersson, E., Arpe, K., Balmaseda, M. A.,

6   Beljaars, A. C. M., Van De Berg, L., Bidlot, J., Bormann, N., Caires, S., Chevallier,

7   F., Dethof, A., Dragosavac, M., Fisher, M., Fuentes, M., Hagemann, S., Hólm, E.,

8   Hoskins, B. J., Isaksen, L., Janssen, P. A. E. M., Jenne, R., Mcnally, A. P., Mahfouf,

9   J.-F., Morcrette, J.-J., Rayner, N. A., Saunders, R. W., Simon, P., Sterl, A.,

10   Trenberth, K. E., Untch, A., Vasiljevic, D., Viterbo, P., and Woollen, J.: The ERA-40

11   Re-Analysis, Quart. J. Roy. Meteor. Soc., 131, 2961–3012, doi:10.1256/qj.04.176,

12   2005.

13   Vega, C. P., Björkman, M. P., Pohjola, V. A., Isaksson, E., Pettersson, R., Martma,

14   T., Marca, A., and Kaiser, J.: Nitrate stable isotopes and major ions in snow and ice

15   samples from four Svalbard sites, Polar Res., 34, 23246,

16   http://dx.doi.org/10.3402/polar.v34.23246, 2015.

17   Vega, C. P., Schlosser, E., Divine, D. V., Kohler, J., Martma, T., Eichler, A.,

18   Schwikowski, M., and Isaksson, E.: Surface mass balance and water stable isotopes

19   derived from firn cores on three ice rises, Fimbul Ice Shelf, Antarctica, The

20   Cryosphere, 10, 2763–2777, doi:10.5194/tc-10-2763-2016, 2016.

21   Vinje, T. E.: Frift av Trolltunga i Weddellhavet, Norsk Polarinstitutt. Arbok, 213 pp.,

22   1975.

23   Wagenbach, D., Ducroz, F., Mulvaney, R., Keck, L., Minikin, A., Legrand, M., Hall,

24   J. S., Wolff, E. W.: Sea-salt aerosol in coastal Antarctic regions, J. Geophys. Res.,

25   103, 10961–10974, 1998.

26   Wagenbach, D., Graf, W., Minikin, A., Trefzer, U., Kipfstuhl, J., Oerter, H., and

27   Blindow, N.: Reconniassance of chemical and isotopic firn properties on top of

28   Berkner-Island, Antarctica. In: Morris, E.M. (Ed.), Ann. Glaciol.: Proceedings of the

29   Fifth International Symposium on Antarctic Glaciology, vol. 20, 307–312, 1994.

30   Weller, R., and Wagenbach, D.: Year-round chemical aerosol records in continental

31   Antarctica obtained by automatic sampling, Tellus, 59, 755–765, 2007.

1 Weller, R., Wagenbach, D., Legrand, M., Elsässer, C., Tian-Kunze, X., and König-
2 Langlo, G.: Continuous 25-yr aerosol records at coastal Antarctica– I: inter-annual
3 variability of ionic compounds and links to climate indices, Tellus, 63B, 901–919,
4 2011.

5 Wendl, I.: High resolution records of black carbon and other aerosol constituents
6 from the Lomonosovfonna 2009 ice core, PhD Thesis, University of Bern,
7 Switzerland, 2014.

8 Wendl, I. A., Eichler, A., Isaksson, E., Martma, T., and Schwikowski, M.: 800-year
9 ice-core record of nitrogen deposition in Svalbard linked to ocean productivity and
10 biogenic emissions, Atmos. Chem. Phys., 15, 7287–7300, doi:10.5194/acp-15-
11 7287-2015, 2015.

12 Wolff, E. W., Jones, A. E., Bauguitte, S. J. B., and Salmon, R. A.: The interpretation
13 of spikes and trends in concentration of nitrate in polar ice cores, based on evidence
14 from snow and atmospheric measurements, Atmos. Chem. Phys., 8, 5627–5634,
15 2008.

16 Yang, X., Pyle, J. A., and Cox, R. A.: Sea salt aerosol production and bromine
17 release: Role of snow on sea ice, Geophys. Res. Lett., 35, L16815,
18 doi:10.1029/2008GL034536, 2008.

19 Yang, X., Pyle, J. A., Cox, R. A., Theys, N., and Van Roozendael, M.: Snow-sourced
20 bromine and its implications for polar tropospheric ozone, Atmos. Chem. Phys., 10,
21 7763–7773, doi:10.5194/acp-10-7763-2010, 2010.

1 **Tables**

2 Table 1. Cores (KC, KM, BI, S100), and snow pits (M1, M2, G3–G5) locations and

3 sampling details. Distances of the core and pit locations to the ice shelf side were

4 obtained using the GIS package Quantarctica (www.quantarctica.org). (*) refers to

5 Kaczmarska et al. (2004), and (§) to Vega et al. (2016).

Site	Location	Elevation	Core length *Ice depth* Ice temp. at 10 m	Distance from the coast	Time coverage	Average SMB
		(m a.s.l.)	(m)	(km)	(years)	(m w.e. y^{-1})
KC§	70°31′S, 2°57′E	264	20.0 *460* -17.5	42	(1958–2012) ± 3	0.24
KM§	70°8′S, 1°12′E	268	19.6 *410* -15.9	12	(1995–2014) ± 1	0.68
BI§	70°24′S, 3°2′W	394	19.5 *460* -16.1	10	(1996–2014) ± 1	0.70
S100*	70°14′S, 4°48′E	48	100 - -17.5	3	(1737–2000) ± 3	0.30
			Snow pit sampling depth (m)			
M1	70°0′S, 1°2′W	55	0.6	21	Aut.2009–2009/11/28	0.38 (for the period 1983–2009 inferred from a composite core, see Vega et al. 2016)
M2	70°19′S, 0°7′W	73	0.7	64	Aut.2009–2009/12/17	
G3	69°49′S, 0°37′W	57	0.9	27	Aut.2009–2009/12/21	
G4(G4a)	70°54′S, 0°24′W	60	0.7	117	Aut.2009–2009/12/19	
G5(G5a)	70°33′S, 0°2′W	82	0.6	83	Aut.2009–2009/12/03	

6

1 Table 2. Median ion concentrations (in μmol L^{-1}) in the KC, KM, BI, and S100 firn/ice

2 cores and in snow pits M1, M2, G3–G5. Ion concentrations at the top 2 m of the KC,

3 KM, and BI cores were not measured. Non-detected concentrations were set as half

4 the detection limit of each ion. Note: (*) the period is 1958.5–2012, (-) not measured.

5 Median values of water stable isotopes and deuterium excess for the KC, KM, and BI

6 are reported by Vega et al. (2016).

Site	Period (years)	Median (μmol L^{-1})								
		MSA	Cl$^-$	Br$^-$ (×10^3)	NO$_3^-$	SO$_4^{2-}$	Na$^+$	K$^+$	Mg^{2+}	Ca^{2+}
KC	1958–2007	0.2	10.0	-	0.6	1.8	9.4	0.2	0.9	0.5
KM	1995–2012	0.3	71.3	-	0.4	4.5	57.7	1.5	6.3	1.6
BI	1996–2012	0.4	23.1	-	0.4	1.9	19.0	0.5	2.0	0.6
S100	1737–2000	0.1	20.9	-	0.5	1.2	20.7	0.4	2.0	0.7
S100	1995–2000	0.1	132.4	-	0.6	3.2	144.0	3.3	10.7	3.0
S100	1737–1949	0.1	16.0	-	0.6	1.0	15.1	0.3	1.4	0.5
S100	1950–2000	0.1	88.5	-	0.5	2.8	98.2	2.0	7.9	1.9
M1		-	55.9	7.5	0.5	2.1	46.4	0.8	5.6	1.2
M2		-	26.2	5.7	0.9	1.2	18.3	0.3	2.7	0.8
G3	aut.2009– sum.2010 for all snow pits	-	27.1	7.1	0.5	1.4	61.9	1.5	6.9	2.0
G4		-	7.4	2.9	0.4	0.4	5.3	0.1	0.7	0.5
G5		-	7.6	3.9	0.4	0.5	5.4	0.2	0.9	0.5
G4a		-	5.6	6.1	0.5	0.3	-	-	-	-
G5a		-	8.1	8.1	0.3	0.4	-	-	-	-

1

Table 3. PCA loadings of the first three (KC) and two (KM, BI, and S100) principal components calculated at an annual resolution in a set of 8 different ions measured in the ice rises and S100 cores. PCA loadings were obtained at three different time intervals in the S100 core: 1737–2000, 1737–1949, and 1950–2000. Sources related to the different components are displayed in the bottom row.

Core	KC			KM		BI		S100					
Resolution	Annual			Annual		annual		annual (1737–2000)		annual (1737–1949)		annual (1950–2000)	
Loadings	PC1	PC2	PC3	PC1	PC2	PC1	PC2	PC1	PC2	PC1	PC2	PC1	PC2
MSA	0.17	0.52	-0.19	-0.20	0.64	0.03	0.65	0.16	0.54	0.23	0.44	0.03	0.73
Cl	0.46	-0.17	-0.19	0.40	0.03	0.43	-0.07	0.42	-0.07	0.43	-0.11	0.42	-0.08
NO₃⁻	0.13	0.59	0.35	-0.26	0.56	-0.03	0.56	-0.06	0.79	-0.08	0.74	0.14	0.60
SO₄²⁻	0.33	0.47	0.08	0.30	0.50	0.30	0.48	0.37	0.23	0.30	0.45	0.38	0.23
Na⁺	0.44	-0.11	-0.22	0.40	0.07	0.43	-0.06	0.42	-0.09	0.43	-0.13	0.42	-0.10
K⁺	0.46	-0.19	-0.11	0.40	0.03	0.40	-0.10	0.41	-0.06	0.41	-0.10	0.42	-0.05
Mg²⁺	0.45	-0.15	0.11	0.39	0.08	0.43	-0.08	0.41	-0.10	0.41	-0.11	0.40	-0.17
Ca²⁺	0.17	-0.24	0.85	0.40	0.10	0.43	-0.03	0.39	0.02	0.36	0.05	0.39	-0.07
Explained Variance (%)	51	22	12	76	18	65	24	70	15	60	17	69	16
Source	sea-salts	biogenic mixed	terrestrial	sea-salts terrestrial	biogenic mixed	sea-salts terrestrial	biogenic mixed	sea-salts terrestrial	biogenic mixed	sea-salts terrestrial	biogenic mixed	sea-salts terrestrial	biogenic mixed

1   Table 4. Correlation coefficients (R) for the median ion concentrations at the different
2   FIS snow pits vs. latitude, longitude, and distance from the ice shelf edge. Numbers in
3   italics show the R values including the ion median concentration values in the KM and
4   BI cores for the year 2009. Significant values at the 95 % confidence interval are shown
5   in bold.

R	Cl^-	Br^-	NO_3^-	SO_4^{2-}	Na^+	K^+	Mg^{2+}	Ca^{2+}
Latitude (˚S)	-0.74	**-0.96**	-0.10	-0.84	**-0.93**	**-0.90**	**-0.90**	**-0.95**
	-0.62	*-*	*-0.07*	*-0.45*	***-0.87***	***-0.83***	***-0.88***	***-0.91***
Longitude (˚W)	0.81	0.67	-0.40	0.77	0.72	0.59	0.57	0.72
	0.16	*-*	*-0.22*	*0.30*	*0.08*	*0.13*	*-0.04*	*0.02*
Distance from the sea (km)	-0.84	**-0.99**	-0.07	**-0.91**	**-0.90**	-0.83	-0.83	**-0.93**
	-0.67	*-*	*0.05*	*-0.64*	*-0.70*	*-0.70*	*-0.61*	*-0.70*

6

1   Table 5. Correlation coefficients (R) for the annual mean chemical concentrations

2   (R_{conc}) and chemical fluxes (R_{flux}) vs. annual snow accumulation in the KC and S100

3   cores. Significant values at the 95 % confidence interval are shown in bold.

R_{conc}	MSA	Cl^-	NO_3^-	SO_4^{2-}	Na^+	K^+	Mg^{2+}	Ca^{2+}
KC	-0.18	-0.17	-0.24	-0.16	0.05	-0.08	-0.21	-0.12
KM	0.14	-0.06	-0.02	0.01	-0.07	-0.04	0.08	-0.04
BI	-0.31	-0.11	-0.57	-0.52	-0.14	-0.19	-0.13	-0.11
S100	0.07	-0.12	**-0.04**	**-0.10**	-0.12	-0.10	**-0.13**	-0.09
S100 (1737–1949)	0.11	-0.11	-0.05	-0.05	-0.11	-0.12	-0.05	-0.05
S100 (1950–2000)	0.16	-0.09	-0.06	-0.10	-0.08	-0.03	-0.15	-0.03
R_{flux}	MSA	Cl^-	NO_3^-	SO_4^{2-}	Na^+	K^+	Mg^{2+}	Ca^{2+}
KC	**0.45**	**0.76**	**0.72**	**0.63**	**0.59**	**0.75**	**0.74**	0.01
KM	**0.59**	**0.65**	**0.57**	**0.71**	**0.64**	**0.68**	**0.74**	**0.73**
BI	0.43	**0.55**	0.42	**0.55**	**0.53**	0.49	**0.56**	**0.73**
S100	**0.18**	0.07	**0.63**	**0.18**	0.08	0.10	**0.16**	**0.13**
S100 (1737–1949)	**0.52**	**0.45**	**0.61**	**0.56**	**0.41**	**0.44**	**0.48**	**0.43**
S100 (1950–2000)	0.22	0.25	**0.73**	0.24	**0.30**	**0.36**	**0.44**	0.27

1   Table 6. Median $nssSO_4^{2-}$ concentrations (in μmol L^{-1}) in the KC, KM, BI, and S100

2   firn/ice cores and in snow pits M1, M2, G3–G5. (-) Not re-calculated.

Site	Period (years)	Median (μmol L^{-1}) $nssSO_4^{2-}$ k=0.06	Median (μmol L^{-1}) $nssSO_4^{2-}$ k'=0.04	Median (μmol L^{-1}) $nssSO_4^{2-}$ k''=0.02
KC	1958–2007	1.1	-	-
KM	1995–2012	0.7	-	-
BI	1996–2012	0.7	-	-
S100	1737–2000	-7×10^{-2}	0.3	0.7
S100	1995–2000	-4.8	-0.9	0.7
S100	1737–1949	0.1	0.4	0.7
S100	1950–2000	-3.1	-0.7	0.7
M1	Aut.2009–Sum.2010 for all snow pits	-0.7	-	-
M2		-0.3	-	-
G3		-3.1	-	-
G4		-2×10^{-2}	-	-
G5		0.2	-	-

3

1   **Figures**

2

3   Figure 1. Satellite image of Fimbul Ice Shelf (FIS) showing the KC, KM, BI, and S100

4   core sites, the M1, M2, G3, G4, and G5 snow pit sites, Jutulstraumen, and Trolltunga.

5   In addition, 50-m contours are shown at each ice rise, as derived from GPS profiles

6   (V. Goel, personal communication, 2016). In addition, the dashed line shows the extent

7   of Trolltunga according to Corona Satellite data from 1963 (J. van Oostveen, personal

8   communication, 2017). Map image is from the MODIS Mosaic of Antarctica

9   (MOA).Map image is from the MODIS Mosaic of Antarctica (MOA). Additional

10   information regarding the sampling sites and traverses in FIS can be found in

11   Schlosser et al. (2014) and Vega et al. (2016).
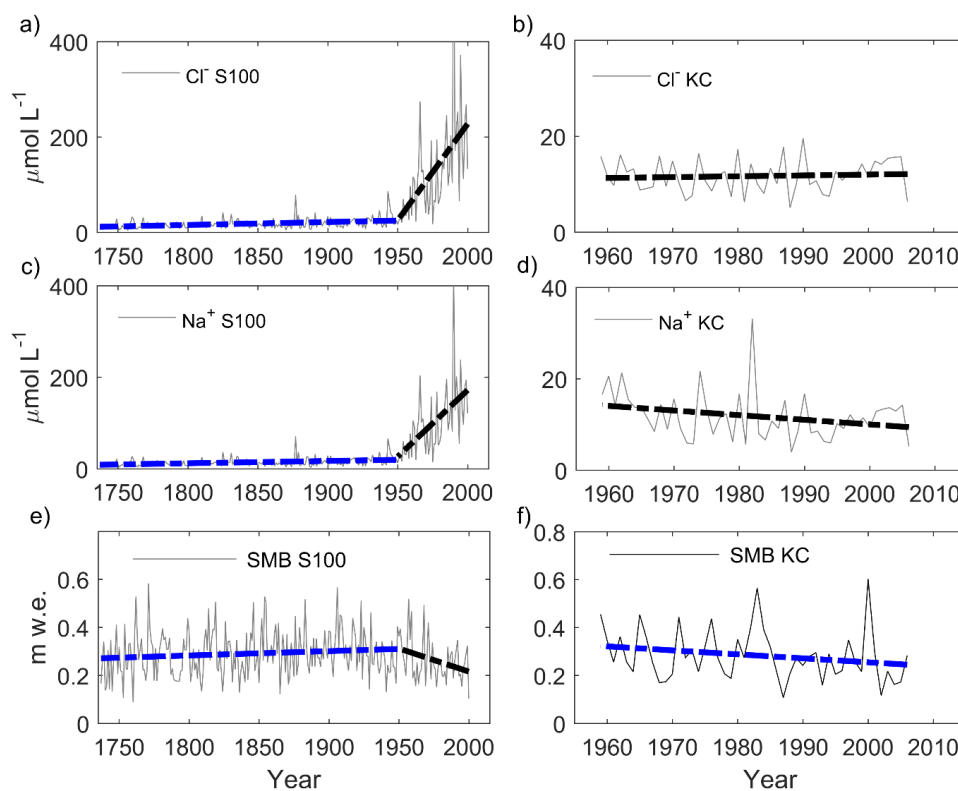
Figure 2. Annual sea-salt (Cl⁻ and Na⁺) concentrations and surface mass balance
(SMB) in the two longest records retrieved at Fimbul Ice shelf, S100, (a), (c), and (e),
and KC, (b), (d) and (f). Linear trends in Cl⁻ and Na⁺ concentration, and SMB measured
in the S100 core are shown for two different periods: 1737–1949 (blue dashed line)
and 1950–2000 (black dashed line) in (a), (c), and (e), respectively. Linear trends in
Cl⁻ and Na⁺ concentrations, and SMB measured in the KC core are shown for the
period 1958–2007 (black dashed line) in (b), (d) and (f), respectively.
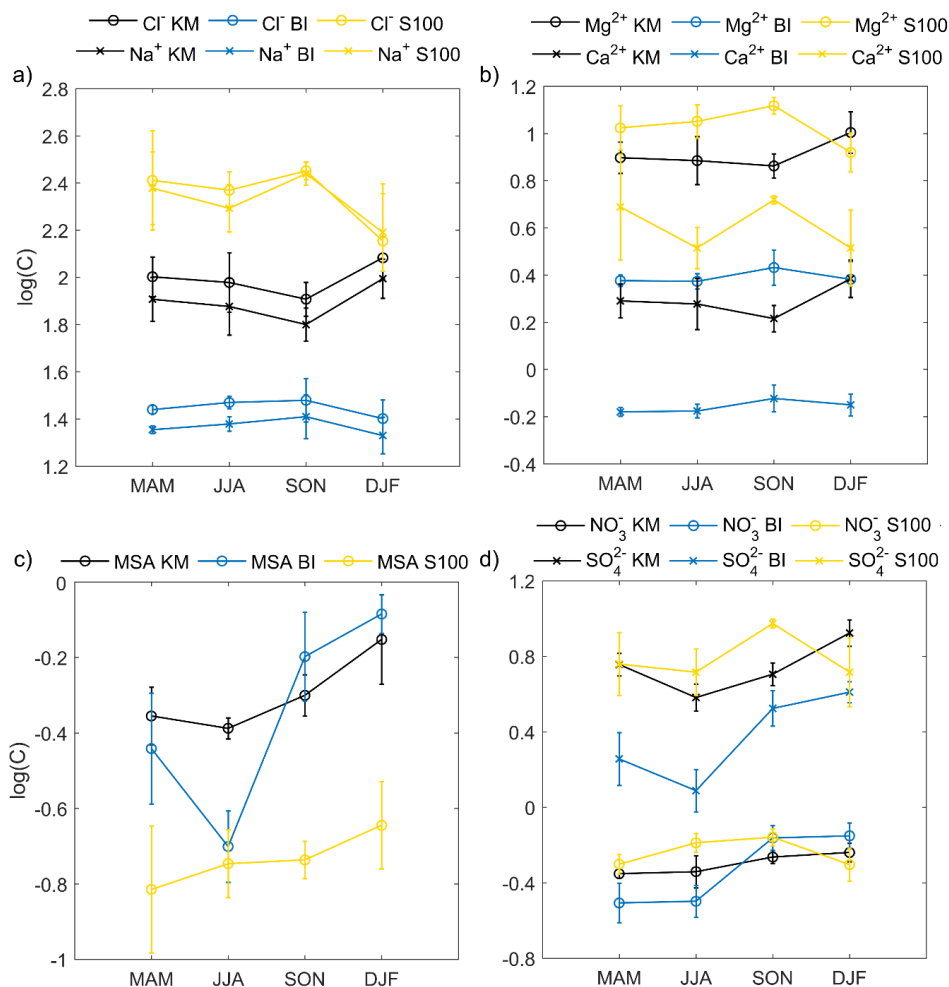
Figure 3. Seasonal variability of selected ions, Cl$^-$ and Na$^+$ (a), Mg^{2+} and Ca^{2+} (b), MSA (c) and NO$_3^-$ and SO$_4^{2-}$ (d) in cores KM, BI, and S100. Average seasonal values were calculated for the trimesters MAM (autumn), JJA (winter), SON (spring), and DJF (summer) from the interpolated composite record (0.01-year resolution) of 16, 15, and 5 years in the KM, BI, and S100 cores, respectively.
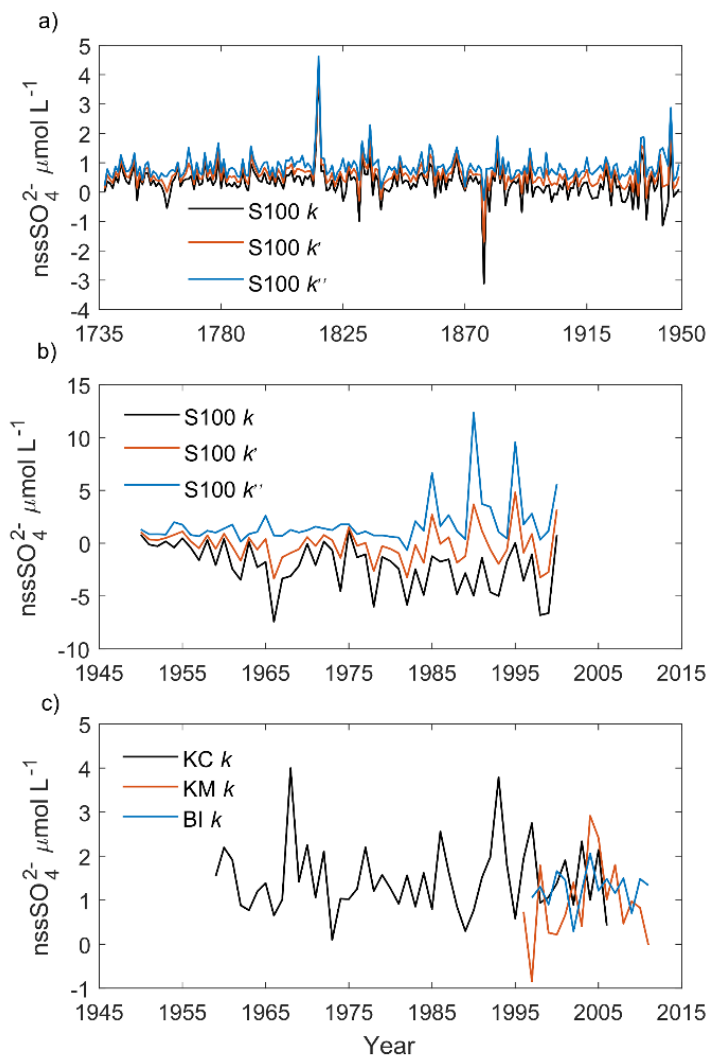
Figure 4. Annual $nssSO_4^{2-}$ concentrations in the S100 core between a) 1737–1949, b) 1950–2000, and c) in the KC, KM, and BI cores. $nssSO_4^{2-}$ recalculated using $k = 0.06$, $k' = 0.04$ and $k'' = 0.02$ are shown in panels a) and b) with black, red and blue lines, respectively. $nssSO_4^{2-}$ in the KC, KM, and BI cores was calculated using $k = 0.06$.
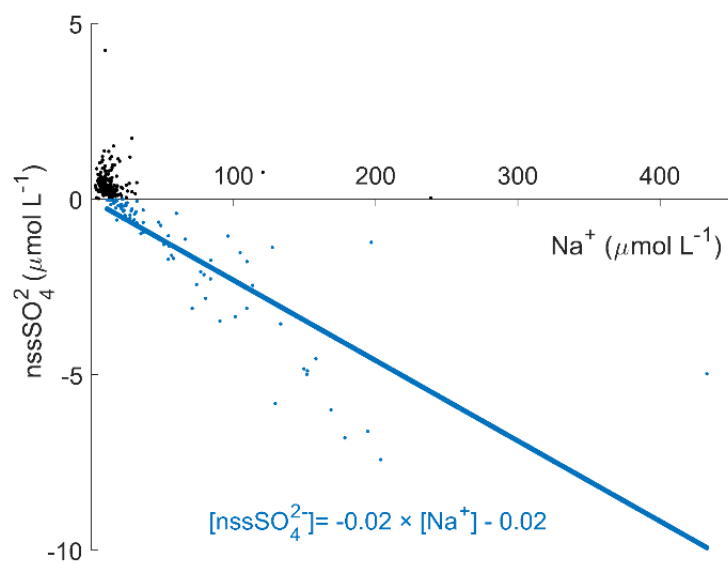
Figure 5. Scatter plot of annual non-sea-salt SO_4^{2-} vs. Na^+ concentrations in the S100 core. $nssSO_4^{2-}$ was calculated using the seawater ratio as described in section 2.3 and using a $k=0.06$ (in $\mu mol\ L^{-1}$). Positive $nssSO_4^{2-}$ values are denoted with black dots, while negative values are denoted with blue dots. A linear regression was calculated using the negative $nssSO_4^{2-}$ values to infer a new value of k, k', following the approach by Inoue et al. (2017).

1
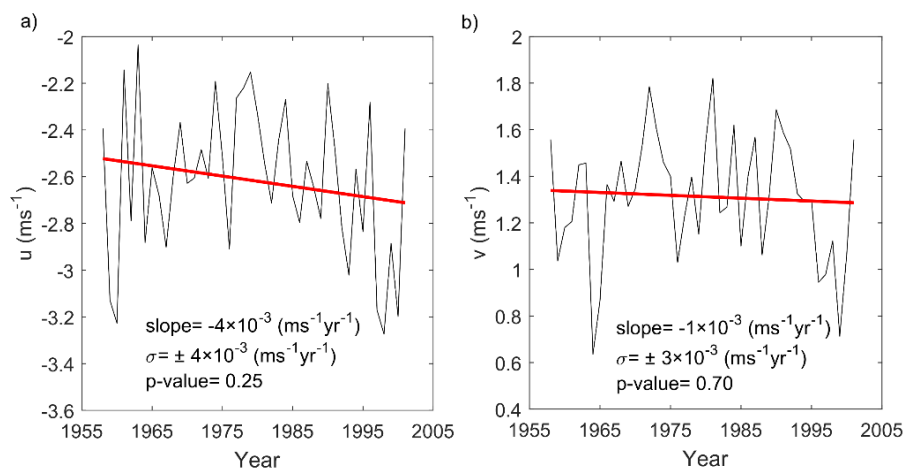
Figure 6. Annual averages of monthly a) zonal, and b) meridional wind speeds (ERA40) for the area (69°S–71°S, 3.5°W–5°E) between 1958–2001. Slope, standard deviation, and *p*-value of the linear regression are shown in the figure.